CORTEX 71 (2015) 377–389

Available online at www.sciencedirect.com

ScienceDirect

Journal homepage: www.elsevier.com/locate/cortex

Research report

Visual processing of optic flow and motor control in the human posterior cingulate sulcus

David T. Field [a,*], Laura A. Inman [a,1] and Li Li [b,**]

[a] Centre for Integrative Neuroscience & Neurodynamics, Department of Psychology, University of Reading, UK
[b] Department of Psychology, The University of Hong Kong, Hong Kong, China

ARTICLE INFO

Article history:
Received 12 January 2015
Reviewed 11 March 2015
Revised 1 July 2015
Accepted 9 July 2015
Action editor Jason Barton
Published online 31 July 2015

Keywords:
Cingulate sulcus visual area
Cingulate sulcus motor area
Self-motion
Optic flow
Posterior cingulate

ABSTRACT

Previous studies have shown that the human posterior cingulate contains a visual processing area selective for optic flow (CSv). However, other studies performed in both humans and monkeys have identified a somatotopic motor region at the same location (CMA). Taken together, these findings suggested the possibility that the posterior cingulate contains a single visuomotor integration region. To test this idea we used fMRI to identify both visual and motor areas of the posterior cingulate in the same brains and to test the activity of those regions during a visuomotor task. Results indicated that rather than a single visuomotor region the posterior cingulate contains adjacent but separate motor and visual regions. CSv lies in the fundus of the cingulate sulcus, while CMA lies in the dorsal bank of the sulcus, slightly superior in terms of stereotaxic coordinates. A surprising and novel finding was that activity in CSv was suppressed during the visuomotor task, despite the visual stimulus being identical to that used to localize the region. This may provide an important clue to the specific role played by this region in the utilization of optic flow to control self-motion.

1. Introduction

Control of self-motion is of fundamental importance. Self-motion generates a specific type of visual information referred to as optic flow, and many studies have sought to identify the cortical network and neural mechanisms associated with the processing of this information. Previous studies of the human posterior cingulate sulcus have revealed that a key part of the network is a bilateral visually responsive region, named cingulate sulcus visual area (CSv), specialised for the processing of optic flow (e.g., Furlan, Wann, & Smith, 2013; Wall & Smith, 2008). This region responds bilaterally even when visual flow is confined to one visual field (Fischer, Bülthoff, Logothetis, & Bartels, 2012). CSv also receives vestibular input (Cardin & Smith, 2011; Smith, Wall, & Thilo, 2012), which is clearly consistent with the proposal that it has a role in the perception and

* *Corresponding author*. Centre for Integrative Neuroscience & Neurodynamics, Department of Psychology, University of Reading, RG6 6AL, UK.
** *Corresponding author*. Department of Psychology, The University of Hong Kong, Pokfulam, Hong Kong, China.
E-mail addresses: d.t.field@reading.ac.uk (D.T. Field), l.a.inman@pgr.reading.ac.uk (L.A. Inman), lili@hku.hk (L. Li).
[1] Tel.: +44 118 3785004.
http://dx.doi.org/10.1016/j.cortex.2015.07.014
0010-9452/

control of self-motion. However, CSv has not been identified in monkeys. Instead, previous studies have identified three motor areas that show somatotopic organization in the banks of the cingulate sulcus of monkeys: a rostral cingulate motor area (CMA) lies inferior to the pre-supplementary motor area, and two caudal CMA's are found ventral to the supplementary motor area – one in the dorsal bank of the cingulate and one on the ventral bank (Amiez & Petrides, 2012; Picard & Strick, 1996). The human homologs of the two caudal CMA's are located close to the reported location of CSv as localised with visual stimuli. For example, Fischer et al. (2012) report the MNI coordinates of CSv at X = −13 ± 3, Y = −26 ± 5, Z = 42 ± 3 in the left hemisphere and X = 13 ± 3, Y = −26 ± 8, Z = 45 ± 3 in the right hemisphere. This may be compared with Picard and Strick's coordinates for 'posterior hand movement region 2' (one of the two human homologues of monkey caudal CMA) at ±X = 7.4 ± 4.2, Y = −29.4 ± 5.8, Z = 48 ± 5.4 for participants whose anatomy lacked the paracingulate sulcus at the location of activation and ±X = 8.9 ± 4.4, Y = −33.4 ± 11, Z = 47.1 ± 7.1 for those whose anatomy did include the paracingulate sulcus. The general location of these visual and motor regions is shown in Fig. 1.

Due to the variability of mean coordinates reported for CSv between studies [e.g., the MNI coordinates for CSv given by Pitzalis et al. (2013) are ±X = 15, Y = −33, Z = 39, Antal, Baudewig, Paulus, and Dechent (2008) give X = −12, Y = −24, Z = 39 and X = 10, Y = −28, Z = 42, while Fischer et al. (2012) give X = −13 ± 3, Y = −26 ± 5, Z = 42 ± 3 and X = 13 ± 3, Y = −26 ± 8, Z = 45 ± 3], it is difficult to compare CSv activations with caudal CMA activations. For example, the reported posterior–anterior location of CSv is sufficiently variable to place it either posterior or anterior to reported caudal CMA coordinates. Existing studies have either used optic flow stimuli aimed at probing the properties of CSv, or simple motor tasks aimed at probing the properties of CMA, but to our knowledge no study has used both types of task as localisers in the same participants. Given this and the spatial resolution of fMRI group results, it still remains in question whether the reported CSv and CMA in the posterior cingulate are two adjacent but separate regions, or a single 'visuomotor' integration region containing both motor neurons and optic flow tuned neurons that interact, or motor neurons that also possess optic flow receptive fields.

The current study is designed to address the above question. Specifically, we used a motor, a visual, and an integrated visuomotor task to localize and differentiate CMA and CSv in the posterior cingulate sulcus in humans. In the motor task participants moved a joystick in response to a tone, and in the visual task they fixated centrally while viewing a changing optic flow field. The visuomotor task used the same visual conditions as the visual task but in addition the participants moved a joystick to track the path trajectory of forward self-motion within the flow field. If CMA and CSv are two separate regions, we would expect to observe contralateral activation in the posterior cingulate for the pure motor task, and bilateral activation that does not overlap with the motor activation for the pure visual task. In the case of the integrated visuomotor task in which optic flow is used to control the parameters of a motor response, activation should occur bilaterally and be the sum of pure visual and pure motor activations. In contrast, if CSv/CMA is a single integration region, we would expect to observe that the pure visual task produces bilateral activation and that the pure motor task produces a contralateral activation that considerably overlaps the visual activation. Under this hypothesis the visuomotor task should produce the same bilateral pattern of activation as the pure visual task.

2. Methods

2.1. Participants

The study had 17 participants (5 male, age range 19–46, mean 24 years), who gave their informed written consent prior to taking part. The study was approved by the University of Reading Research Ethics Committee. Nine participants performed the motor and the visuomotor tasks right-handed, and eight left-handed. All participants performed the visual task.

2.2. Tasks and stimuli

Three tasks were used in the current study. The motor task was based on that used by Deiber et al. (1991) to localize CMA. The task had two conditions: in the Fixed condition, a tone was presented to participants every 2 sec, and participants were instructed to move a MAG Design and Engineering MRI

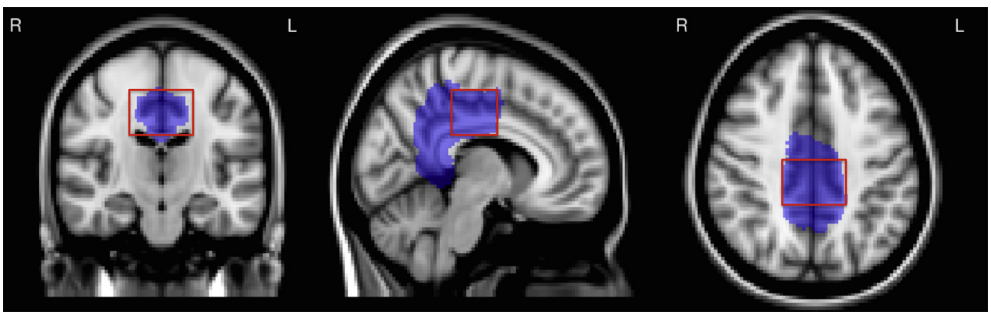

Fig. 1 – The 'cingulate gyrus posterior division' mask taken from the Harvard Oxford Cortical Structural Atlas is shown in blue on coronal, sagittal, and axial slices of the MNI template brain. In this study statistical analysis of functional voxel time courses was restricted to voxels inside this mask. The part of the posterior cingulate where regions CSv and CMA have been reported is indicated by the red squares. See Method for details.

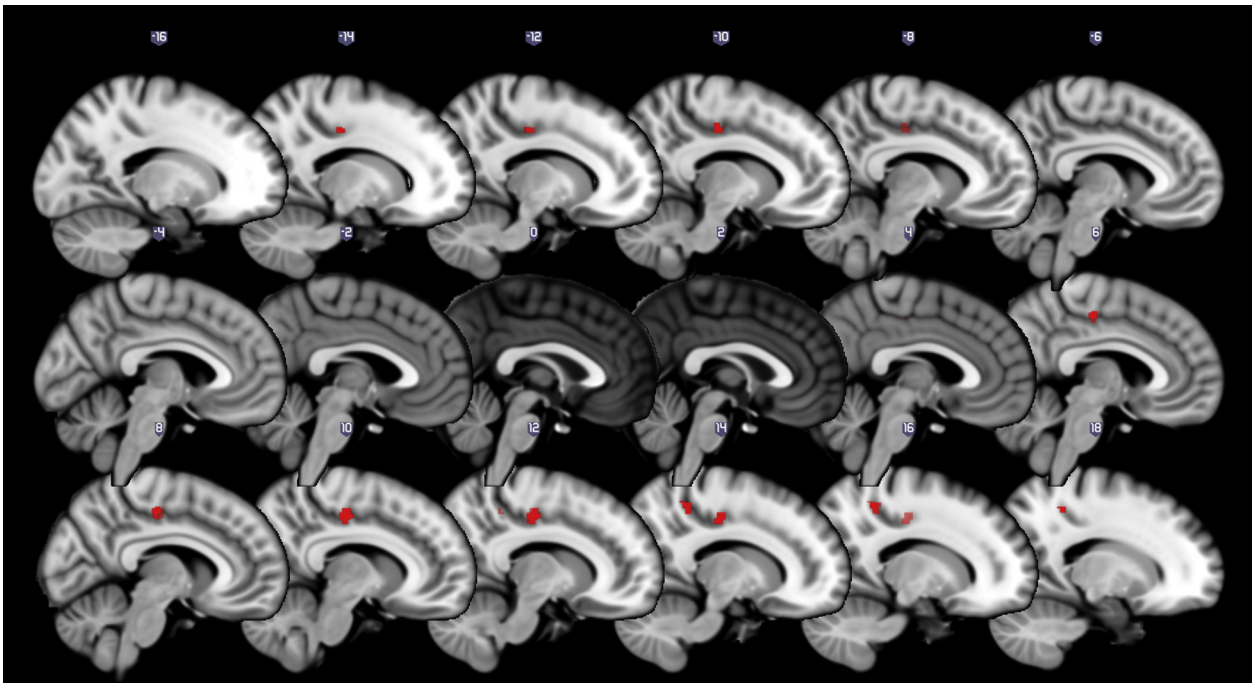

Fig. 2 – Sagittal slices from the MNI standard brain at 2 mm intervals with voxels more activated by viewing coherent optic flow than scrambled flow highlighted in red. The bilateral red activation in cingulate sulcus is the area known as CSv. The contrast also revealed a more anterior and posterior activation in the cingulate sulcus that only appeared in the right hemisphere. The range of slices displayed was chosen to not omit any active voxels that fell within the posterior cingulate mask. Numbers indicate slice position in mm, with negative numbers corresponding to the left hemisphere.

compatible joystick forwards as soon as they heard the tone. In the Random condition, a different tone from that used in the Fixed condition was presented to participants every 2 sec, and participants were instructed to move the joystick either forwards, backwards, left, or right, with the constraint that they should not produce long sequences of the same movement or repetitive patterns. Before scanning, half of the participants were trained to perform the Fixed task in response to low pitched tones, and to perform the Random task in response to high pitched tones. The other half of the sample was trained using the opposite mapping. Given Deiber et al. (1991) results, we expected both conditions of the motor task to activate CMA, with potential for stronger activation in the random condition. In both conditions, participants kept their eyes closed and a 16 sec block was composed of 8 trials (tones). Eight Fixed and eight Random blocks were presented in the same scan session, interleaved with rest periods. A double length rest period was included in the middle of the sequence to prevent the experimental signal from becoming correlated with the low frequency periodic noise present in the BOLD time series. The total duration of the scan session was 445.89 sec (167 TR).

The visual task was used to localize CSv. It has been reported that CSv responds particularly strongly to coherent optic flow of the type produced during self-motion (Antal et al., 2008; Fischer et al., 2012; Wall & Smith, 2008). The visual task thus involved passive viewing of this type of flow field.

In the same scan session as the visual task, a visuomotor task was used to examine the activation produced when optic flow is used to control motor-output. The visual stimulus for this task was identical to that for the visual task, but a motor task was introduced in which participants moved the joystick left and right to track the path trajectory of forward self-motion specified by optic flow in the visual display. This task was performed in an open-loop manner, without visual feedback of success of tracking. Sixteen sec blocks of the visual and the visuomotor tasks were interleaved with fixation-only rest periods, where a static random dot cloud was presented. The temporal structure of the block design was the same as that detailed above for the motor task. Participants fixated a central cross when performing both tasks. The optic flow presented in each block was produced by simulation of travelling at 21 m/sec along one of eight different courses through a 3D random dot cloud. This visual stimulus was produced using Vizard 3.0 to simulate a virtual 3D environment of dimensions 120 × 40 × 1000 m populated by 30,000 randomly distributed dots. The viewpoint (i.e., virtual line of sight) traversed a winding path along the long axis of the environment, which was produced by summing sine waves of different frequencies and amplitudes. The viewpoint was continuously rotated to be aligned with the instantaneous heading direction, and consequently the flow field contained rotation indicating the curvature of the travelled path (see Li & Cheng, 2011). Note that in displays such as this one, which simulate common everyday locomotor scenarios, a focus of expansion in the flow field indicating instantaneous heading is not present. The view was near-clipped at .5 m and far-clipped at 80 m. As a result of this clipping in combination with the dimensions of the visual display that formed the

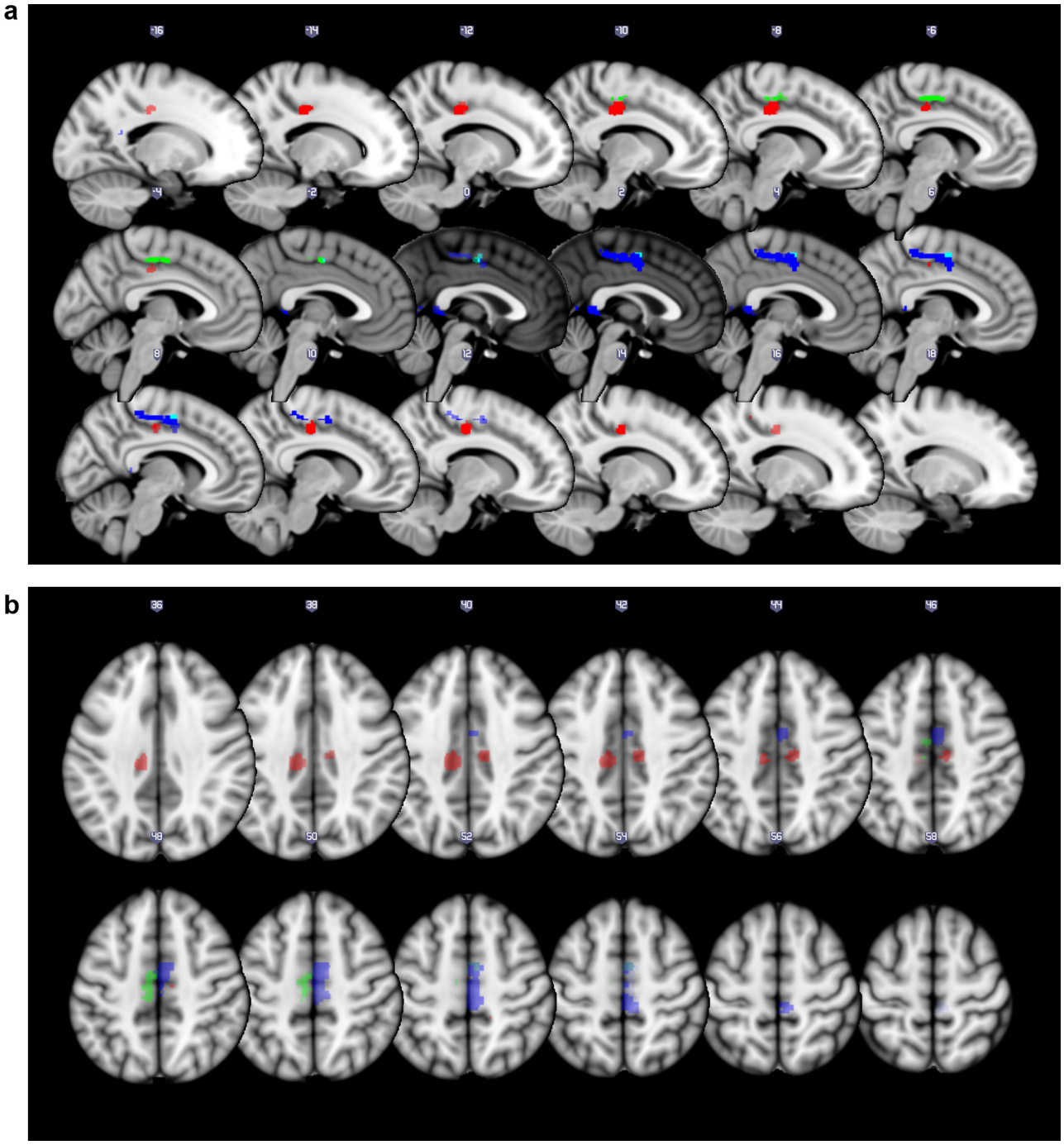

Fig. 3 – Voxels more activated by viewing coherent optic flow than by the rest condition (CSv) are highlighted in red (sagittal slices in 3a, transverse slices in 3b). Voxels more activated by moving the joystick (CMA localiser) than by the rest condition are highlighted in green (right hand group) and blue (left hand group). Some voxels (cyan) near the midline were activated by both right and left hand versions of the CMA localiser. Note that despite the close proximity of the CMA and CSv activations, there were no voxels active in both localizers. For other details see Fig. 2.

viewport on the virtual environment, approximately 100 dots were visible at any given moment. To produce the block design the viewpoint stopped moving after 16 sec and paused for 16 sec before moving again. This resulted in an alternation between static dot fields and optic flow and also meant that the optic flow experienced in each block represented a different course of travel. The visual stimuli were presented to participants with a NordicNeuroLab VisualSystem at 60 Hz on two 600 × 800 pixel LED screens (optically fused by the observer), which subtended 30 (H) × 23° (V) in visual angle.

To confirm our localization of CSv, we also modified the flow field to produce a randomised scrambled flow pattern.

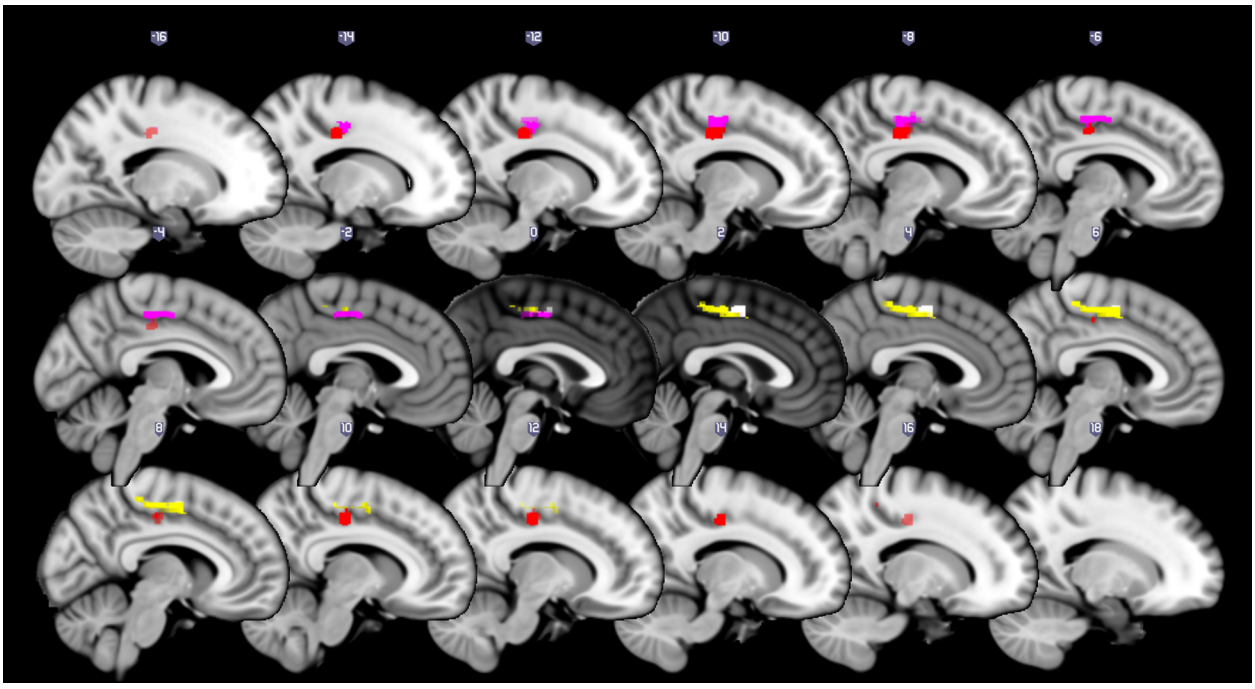

Fig. 4 – Voxels more activated by viewing coherent optic flow (CSv) than by the rest condition are highlighted in red. Voxels more activated by viewing coherent optic flow while tracking the changing heading specified by optic flow with a joystick than by the rest condition (visuomotor localiser) are shown in magenta (right hand) and yellow (left hand). Some voxels (white) near the midline were activated by both right and left hand versions of the visuomotor task. Given the use of optic flow by participants in the visuomotor task, it is surprising that there was no overlap between CSv and the visuomotor activations, which are essentially the same areas activated by the CMA localiser (see Fig. 3). For other details see Fig. 2.

This pattern is known to strongly activate classical visual motion selective areas such as MT and MST, but produces minimal or zero activation in CSv (Antal et al., 2008; Fischer et al., 2012). This stimulus was produced in Vizard 3.0 by moving the dots in the virtual environment while keeping the viewpoint stationary. Each dot was randomly assigned a direction of motion in each of the X, Y, and Z dimensions. Dots at different depths in the virtual environment had different translation speeds in the visual display. The total number of dots visible at any given time approximated 100 – the reduction in visible dots over time due to dots moving off the display was compensated for by dots that were not initially visible on the display moving onto it.

The scrambled flow stimulus was passively viewed in a separate scan session, interleaved with fixation-only rest periods where a static dot field was presented. The total duration of the scan session for the scrambled flow pattern was 293.7 sec (110 TR).

We noted in a pilot study that BOLD signals in the posterior cingulate caused by the visual task were relatively weak; therefore to increase confidence in our findings we included a replication of the key scan session that contained both the visual and the visuomotor task. The replication scan differed in one respect, which was that optic-flow information was generated by simulated self-motion over a textured ground plane rather than through a 3D random dot cloud. A ground plane is a more ecologically valid stimulus than a cloud of random dots that provides the same visual information. Details of the ground-plane stimulus have been fully described previously (see Field, Wilkie, & Wann, 2007).

2.3. *Imaging acquisition parameters*

Imaging data were acquired at the University of Reading (Centre for Integrative Neurosceince and Neurodynamics) using a Siemens Allegra 3T scanner. Functional scans consisted of repeated single-shot echo-planar imaging (EPI): echo time (TE) = 30 msec, flip angle (FA) = 90°, matrix size = 64 × 64, field of view (FOV) = 192 × 192 mm^2, with slice order descending and interleaved, 50 slices (0 inter-slice gap), slice thickness = 3.0 mm, and repetition time (TR) = 2670 msec. A detailed T-1 weighted MPRAGE anatomical image (resolution1 mm^3) was acquired (TR = 2020 msec, TE = 2.52 msec, FA = 9, FOV = 250 × 250 mm^2, 176 slices, no gap, total scan time = 4 min and 34 sec). A gradient field map was acquired and used to unwarp the EPI scans (50 slices, voxel size = 3 mm^3, TR = 529 msec, TE1 = 4.92 msec, TE2 = 7.38 msec).

2.4. *Data analysis*

2.4.1. *FMRI*

FMRI data processing was carried out using FEAT (FMRI Expert Analysis Tool) Version 6.00, part of FSL (FMRIB's Software Library, www.fmrib.ox.ac.uk/fsl). The following pre-statistics processing was applied: distortion correction using BO

unwarping, motion correction using MCFLIRT (Jenkinson, Bannister, Brady, & Smith, 2002); slice-timing correction using Fourier-space time-series phase-shifting; non-brain removal using BET (Smith, 2002); spatial smoothing using a Gaussian kernel of FWHM 6 mm; grand-mean intensity normalisation of the entire 4D dataset by a single multiplicative factor; highpass temporal filtering (Gaussian-weighted least-squares straight line fitting, with sigma = 42.5 sec for the CMA localiser and visual/visuomotor scans and with sigma = 25.0 sec for the scrambled flow scan). Registration to high resolution structural and standard space MNI template images was carried out using FLIRT (Jenkinson & Smith, 2001; Jenkinson et al., 2002). Registration from high resolution structural to standard space was then further refined using FNIRT nonlinear registration (Andersson, Jenkinson, & Smith, 2007a, 2007b).

The BOLD response was modelled using the GLM and a design matrix of explanatory variables (EVs) derived from the time course of the experimental stimuli, convolved with the standard FEAT double gamma HRF function. Temporal derivatives of the EVs were also included in the design matrix. EVs were high pass filtered in the same way as the data. Time-series statistical analysis of individual participant data was carried out using FILM with local autocorrelation correction (Woolrich, Ripley, Brady, & Smith, 2001). Analysis was *a-priori* restricted to voxels contained within a mask defined by the Harvard Oxford Cortical Structural Atlas 'cingulate gyrus posterior division', available within FSL. Statistical analysis to determine group average activations was conducted with FSL using FLAME 1 and 2 (Behrens, Woolrich, & Smith, 2003). Z (Gaussianized T/F) statistic images were thresholded voxel-wise using $Z > 1.96$ uncorrected for multiple comparisons, corresponding to a two-tailed alpha of .05. This threshold is relatively lenient compared to those used in typical whole brain fMRI studies, but was justifiable because our anatomical region of interest was restricted a-priori using the above anatomical criteria. In practice this method adequately revealed clear function-structure correspondences in an area of the brain where the BOLD signal is relatively weak, without obvious noise being present. As a further safeguard against the risk of reporting false positive activations (given the lenient threshold) we replicated key contrasts in a separate scan that was identical in all respects to the main experimental scan apart from low level visual differences in how optic flow was generated, as described above. Patterns of results that appear in both versions of the experiment are highly unlikely to represent spurious activation.

2.4.2. *Region of interest analysis*

The group average activation maps indicated clearly that CSv and CMA are different regions. Therefore, to provide a more quantitative evaluation of the BOLD response under the different conditions of the experiment we defined regions of interest (ROI) in individual subjects for CSv, CMA, and also MT+. We included MT+ to provide a reference point for interpreting the pattern of responses observed in CSv. The region of interest approach also allowed us to address the anatomical question concerning the relative locations of CSv and CMA at the individual as well as the group level. To avoid circularity we used independent data for ROI definition and response amplitude estimation. CSv was localised using the visual condition data in which optic flow was provided by a dot cloud, relative to rest. MT+ was localised using the same contrast. CMA was localised using the fixed version of the motor task. For all 3 regions we extracted percent signal change for visual, visuomotor and motor conditions. To avoid circularity percent signal change was calculated from the ground plane version of the experiment in the two former cases and using the random version of the motor task in the latter case.

To define the regions of interest in each subject, we first defined CMA (either left or right) by applying an appropriate Z threshold to the fixed motor task contrast, and then defined CSv in both hemispheres by using a separate (generally lower) threshold applied to the visual task contrast. Choice of appropriate threshold was informed by viewing contrast images from individual participant data overlaid on individual subject anatomy, with both images registered to the MNI template and overlaid on the posterior cingulate mask (Fig. 1). We tried to ensure that both regions fell within the posterior cingulate mask, with the focus of CSv in the fundus of the cingulate sulcus as previously reported and the focus of CMA in the dorsal bank of the sulcus. The threshold applied to the visual task contrast was then further adjusted as necessary (generally increased) to isolate MT+ bilaterally in each subject.

2.4.3. *Joystick tracking task*

To verify that participants could accurately track changes in their path trajectory of forward self-motion using the joystick when performing the visuomotor task, the joystick x-position data were analysed using the same method as Billington, Field, Wilkie, and Wann (2010). Briefly, the rate of change of the joystick position (60 samples per sec) was rescaled to match the range of the rate of change of angular heading, enabling the two time series to be plotted on the same graph. The temporal accuracy of tracking was quantified using cross-correlations of the actual heading with the joystick position across a range of plausible lags. The maximum cross-correlation lag provides an estimate of the temporal tracking lag between the joystick position and what is displayed on the screen at that moment.[2] The extent to which participants were able to track the heading changes in their joystick responses was assessed by the R^2 value of the fit of the joystick

[2] Note that this is not equivalent to the lag between perception of the visual information on the display and the perception of the joystick position. One reason for this is that the estimate does not adjust for system delays inherent in the joystick and the recording computer (approximately 100 msec lag compared to the screen). Secondly, perception of the optic flow is lagged relative to its presentation on the screen; the delay in processing optic flow for the extraction of heading direction is in the range 300–430 msec. (Crowell, Royden, Banks, Swenson, & Sekuler, 1990; Hooge, Beintema, Van Den Berg, 1999). On the other hand, perception of joystick position is not subject to such lags because it is under participant control and therefore efference copy signals and internal forward models provide for an accurate real time estimate of position (Miall & Wolpert, 1996). Taking both these factors into account, the cross-correlation method is likely to over-estimate the perceptual lag between the screen and the joystick by approximately 500 msec. However, these factors do not affect the interpretation of the corresponding R^2 values.

positions at the chosen lag to the heading changes. In this experiment, each participant experienced eight different courses of travel. Here, the analysis is presented for one representative course in Fig. 5.

3. Results

3.1. Localization of CSv and CMA

The visual task that involved passive viewing of optic flow produced a bilateral activation in the posterior cingulate compared with fixation of a static flow field. To confirm that the activation was specific to optic flow rather than simply related to visual stimulation we performed a group average analysis subtracting the scrambled flow condition from the optic flow condition. Bilateral activation survived the contrast (Fig. 2), replicating previous findings and confirming that we were successful in localizing CSv.

The Fixed and Random conditions of the motor task produced near identical activation in the posterior cingulate, and therefore we combined the results from these two conditions at the 2nd level of our GLM analysis. As expected, the motor task produced activation in the posterior cingulate contralateral to the hand used to move the joystick and was thus successful in localizing CMA. The locations of the CMA activations are shown on sagittal and transverse slices in Fig. 3, along with the locations of the CSv activations produced by viewing optic flow compared to rest. Peak activation coordinates for CSv and CMA are given in Table 1. The CMA activations and the CSv activations do not overlap, which indicates that they are separate functional areas, and that the alternative hypothesis of a single integrated visuomotor region in the posterior cingulate is false. CSv lies in the fundus of the cingulate sulcus as originally reported, while CMA lies in the dorsal bank of the sulcus and is more extensive than CSv in the anterior–posterior dimension, as well as extending further towards the medial surface. Fig. 7, showing the locations of CMA and CSv ROIs in four individual subjects confirms that this is the case, although CMA is only seen to be more extensive in the anterior–posterior dimension in two of the four cases.

3.2. Responses of CMA and CSv during the visuo-motor task

Given that the visual and the motor tasks indicated two separate regions (CSv and CMA) in the posterior cingulate, we expected that the visuomotor task would activate both regions – CSv bilaterally and CMA contralaterally to the hand used to control the joystick. Fig. 4 shows that the visuomotor task did activate CMA in the expected way, but unexpectedly failed to activate CSv – even at the liberal statistical threshold employed here. Peak activation coordinates are given in Table 1. The observed suppression of optic flow related activation in CSv during the visuomotor task has not previously been found in other flow sensitive areas such as MT+, which respond strongly under visuomotor conditions similar to those used here (Billington et al., 2010; Field et al., 2007). To confirm this functional dissociation between MT+ and CSv in the present data we included MT+ in the region of interest (ROI) analysis (see Section 3.4).

3.3. Replication using the ground plane visual display

The ground plane stimulus scan included both the visual task where the flow field of the ground plane was viewed passively and the visuomotor task in which participants tracked

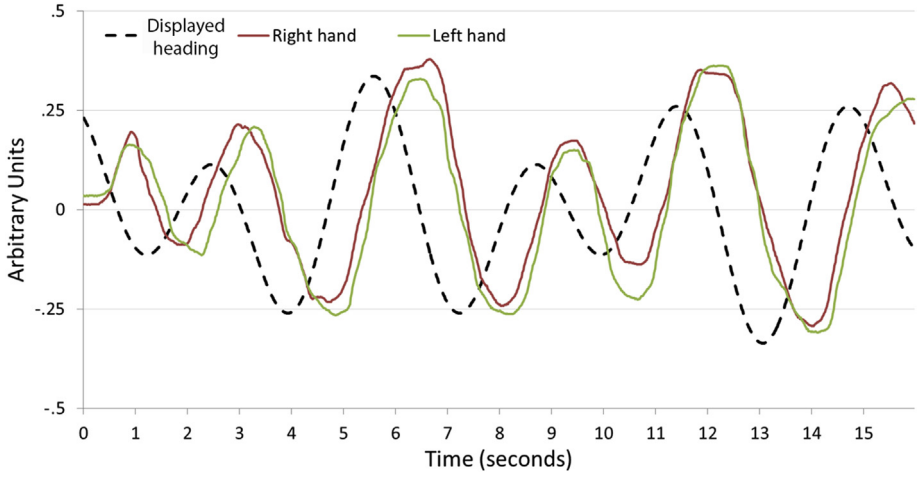

Fig. 5 – Behavioural responses averaged across participants for a representative course used in the visuomotor task. Changes in displayed heading direction are indicated by the black dashed line, the average right handed response is indicated by the red line the left handed response is indicated by the blue line. In the right hand condition, joystick responses lagged the display by .76 sec on average (95% CI .68–.84 sec) compared to .75 sec in the left hand condition (95% CI .63–.86 sec) – but note that these values have not been adjusted for several factors that would act to reduce the true perceptual lag, see method for details. The overall fit between participants' tracking responses and the display was good, although slightly worse in the left-handed condition. The mean R^2 right-handed was .87 (95% CI .84–.90) and .80 left-handed (95% CI .75–.84).

Table 1 – Peak activation coordinates produced by functional contrasts employed in this study.

Functional contrast	Brain region	Peak z	MNI coordinates		
			X	Y	Z
Visual task – baseline	CSv right	4.34	10	−20	40
Visual task – baseline	Csv left	4.26	−10	−26	38
Visual task – scrambled flow	CSv right	3.97	12	−20	44
Visual task – scrambled flow	Csv left	3.21	−12	−22	40
Visual task (ground plane) - baseline	CSv right	3.72	14	−16	44
Visual task (ground plane) - baseline	Csv left	2.64	−12	−18	38
Motor task (left hand) - baseline	CMA right	3.34	4	−10	52
Motor task (right hand) - baseline	CMA left	3.19	−8	−14	52
Visuomotor (left hand) - baseline	CMA right	4.35	4	−10	52
Visuomotor (right hand hand) - baseline	CMA left	3.92	−8	−14	52
Visuomotor (ground plane, left hand) - baseline	CMA right	3.06	4	−8	54
Visuomotor (ground plane, right hand) - baseline	CMA left	3.13	−6	−14	46

changes in the heading specified by optic flow using a joystick. Fig. 6, which presents the results, is therefore directly comparable with Fig. 4. The two figures are strikingly similar, confirming the unexpected finding that passive viewing of optic flow stimuli activates CSv, but that heading tracking with a joystick using the same visual stimulus does not. Activation coordinates may also be compared in Table 1.

3.4. *Region of interest analysis*

We successfully identified CSv in 31 out of 34 hemispheres. CMA was identified in 16 out of 17 hemispheres. MT+ was identified in 33 out of 34 hemispheres, and the average location of MT+ was in agreement with previous anatomical studies (Dumoulin et al., 2000), as well as previous functional studies from our own lab (Moutsiana, Field, & Harris, 2011). Descriptive information about the size and anatomical location of the ROI's is provided in Table 2. ROIs from four example participants are overlaid on individual anatomy in Fig. 7. Percent signal change for each task in each region is plotted in Fig. 8, and confirms the patterns suggested by the group analysis. Specifically, CMA responds strongly in motor and visuomotor conditions, but not the visual condition, while CSv responds in the visual condition and does not respond in the

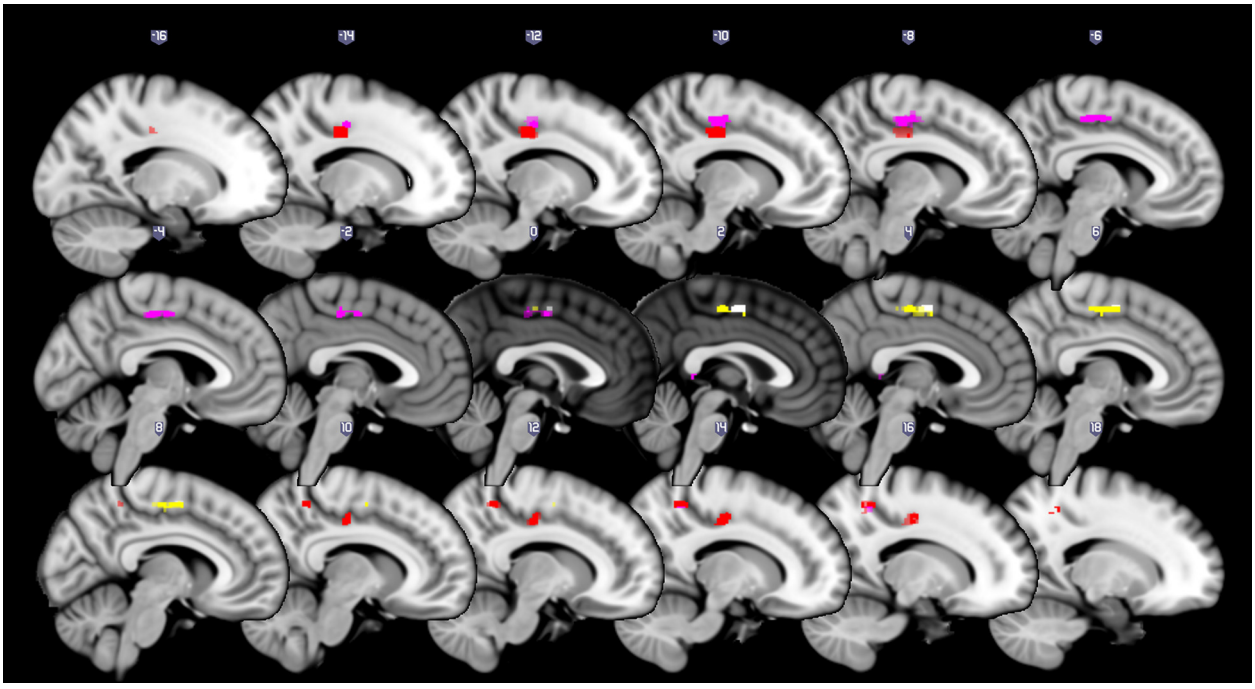

Fig. 6 – Voxels more activated by viewing simulated self-motion over a ground plane (CSv) than by the rest condition are highlighted in red. Voxels more activated by viewing the ground plane while tracking the changing heading specified by optic flow with a joystick movement (visuomotor localiser) than by the rest condition are shown in magenta (right hand) and yellow (left hand). Some voxels (white) near the midline were activated by both right and left hand tracking in the visuomotor task. The pattern of activations is strikingly similar to that in Fig. 4 (optic flow provided by a 3D random dot cloud rather than a ground plane), and replicates the surprising finding that there is no overlap between CSv and visuomotor activations that are essentially the same areas as CMA activations (see Fig. 3). For other details see Fig. 2.

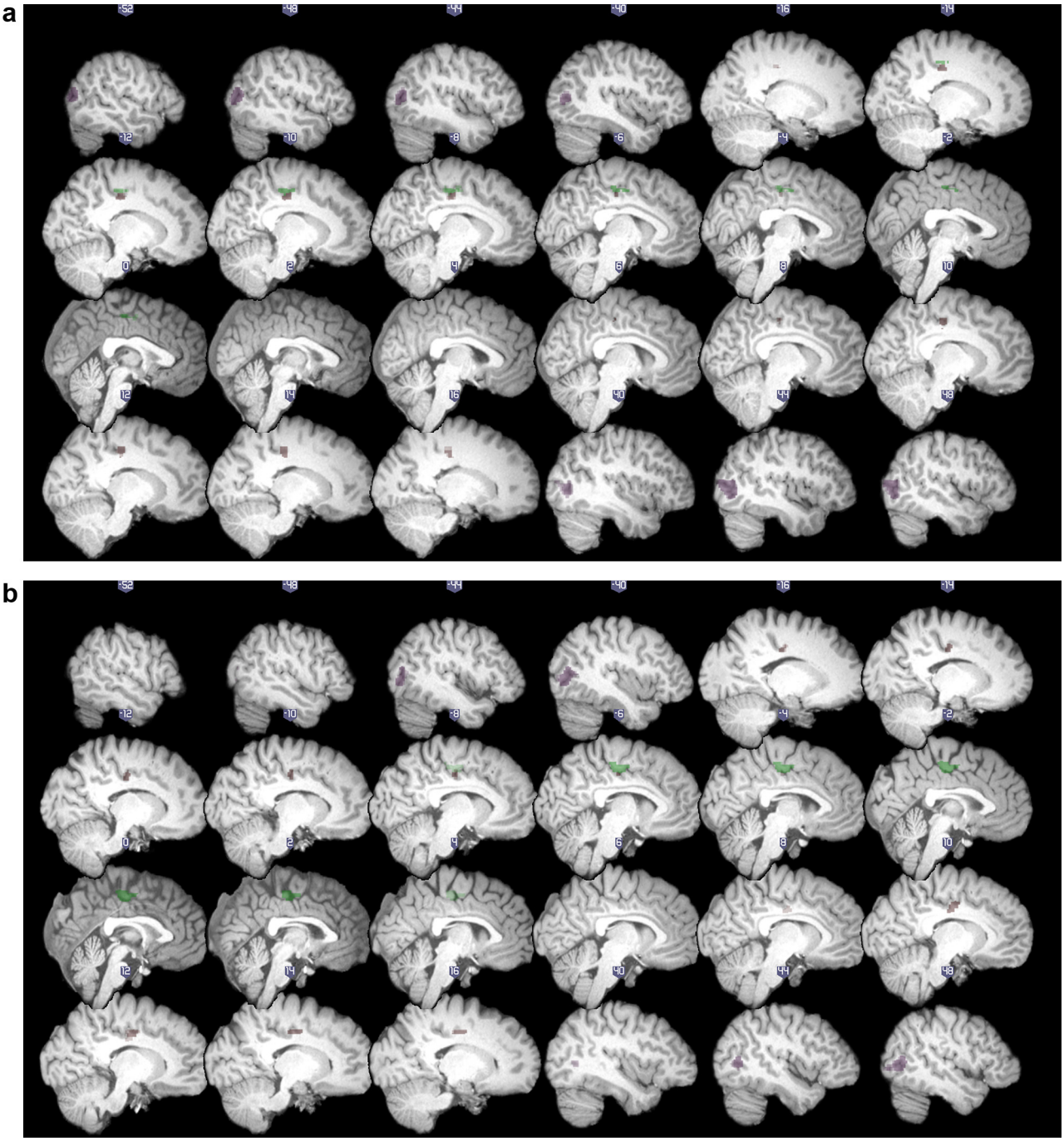

Fig. 7 – Region of interest masks from four representative participants created using the same contrasts presented as group averages in Fig. 3. Participants who performed the motor tasks right handed are shown in 7a and 7b, left handed in 7c and 7d. See Method for details of how thresholds were selected for the purpose of mask definition. Region MT+ is highlighted in purple; CSv is highlighted in red; left CMA in green; and right CMA in blue.

motor condition but surprisingly also fails to respond in the visuomotor condition. The dissociation between the visual and visuomotor conditions found in CSv is not reflected in MT+, which responds equally vigorously in both visual and visuomotor conditions and does not respond during the motor task. We confirmed these observations statistically using a 3 (region: CSv *vs* CMA *vs* MT+) × 3 (task: Visual *vs* Visuomotor *vs* Motor) mixed ANOVA. This produced highly significant main effects of region [$F(2,77) = 9.3$, $p < .001$] and task [$F(2,154) = 9.7$, $p < .001$], as well as a highly significant interaction [$F(4,154) = 38.5$, $p < .001$]. To statistically confirm that CSv and MT + differ in their pattern of response across the visual and visuomotor tasks we first computed a difference score (visual response − visuomotor response) for both ROIs. This had the effect of removing the large difference in overall signal change levels between the two regions from the data,

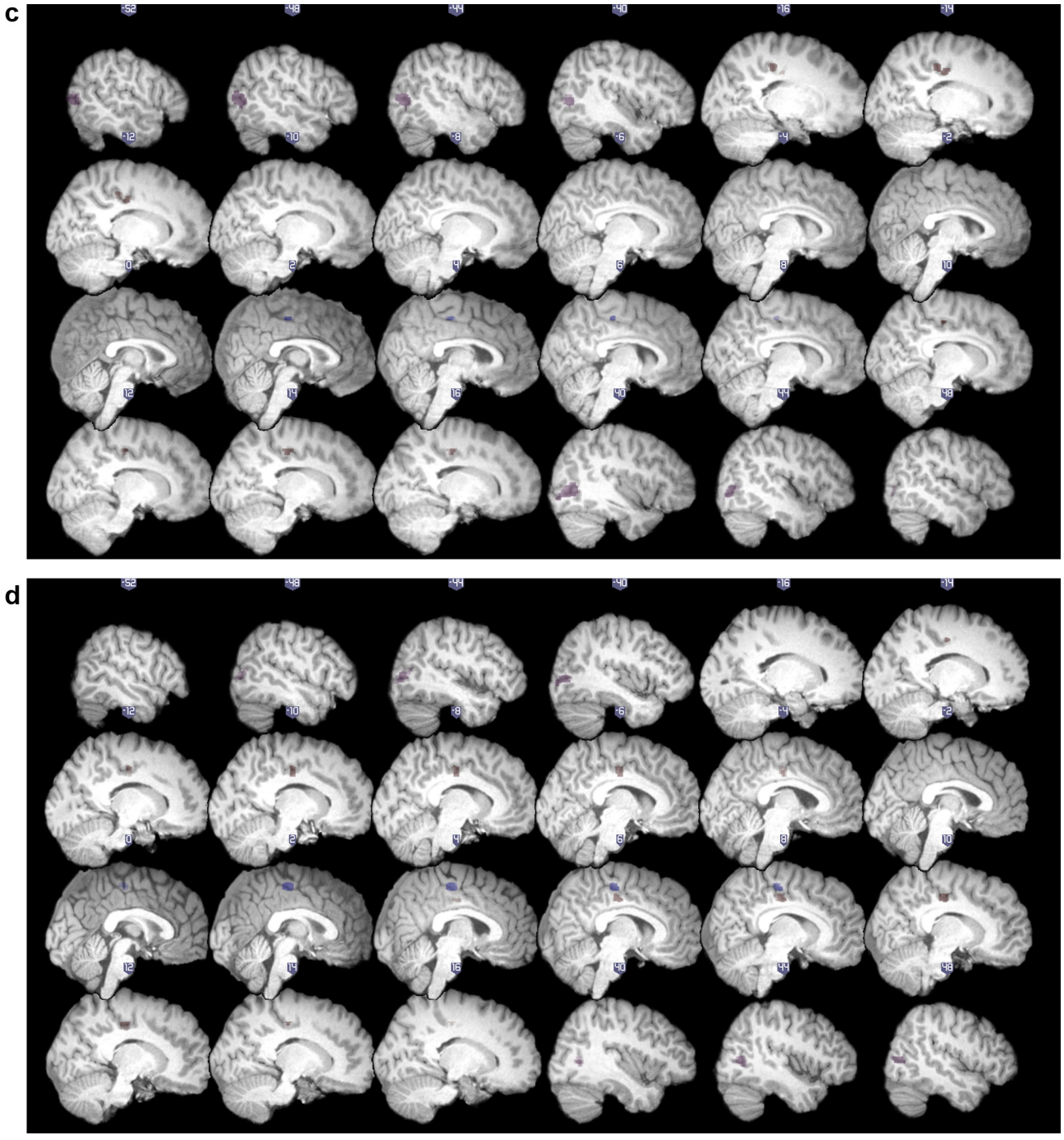

Fig. 7 – (*continued*).

which in any case is unlikely to be neural in origin. As expected, the difference scores were positive in CSv (mean .150%) and close to zero in MT+ (mean .016%), and a paired *t* test confirmed that the two regions differed reliably [$t(30) = 2.4$, $p = .02$].

4. Discussion

We found that CMA and CSv are separate functional brain regions that are close neighbours in stereotaxic space. However, considering the grey matter as a folded sheet the two areas have very distinct locations – CSv is located in the fundus of the cingulate sulcus and CMA lies on the dorsal bank of the sulcus and extends further towards the medial surface as well as being much more extensive than CSv in the anterior–posterior dimension. The possibility that CMA and CSv together comprise a single visuomotor integration region was firmly rejected by the data at both the group and individual level. However, we unexpectedly discovered that visual responses in CSv are suppressed when participants manually control a joystick using the same optic flow information that

Table 2 – Mean locations and sizes of individual participant region of interest masks. Standard deviations are given in brackets.

Brain region	Mean size (voxels)	MNI coordinates of peak voxel		
		Mean X	Mean Y	Mean Z
CSv right	19.6 (9.8)	11.9 (2.8)	−17.2 (4.9)	44.4 (4.3)
CSv left	25.7 (15.6)	−10.9 (2.6)	−22.9 (5.1)	41.9 (4.7)
CMA right	32.7 (11.6)	5.4 (2.8)	−21.1 (7.3)	54.6 (6.2)
CMA left	40.6 (21.39)	−5 (2.4)	−18.3 (5.5)	51.5 (2.6)
MT+ right	82.8 (5.0)	45.8 (3.6)	−74.9 (3.8)	6.3 (5.2)
MT+ left	65.6 (34.0)	−45.4 (3.9)	−73.9 (3.8)	5.75 (6.5)

typically drives visual responses in CSv, and this in itself may be suggestive of a form of visual/motor interaction occurring in CSv. We confirmed that the suppression was specific to CSv by comparing the BOLD responses in MT+, which shows no such suppression.

4.1. *Methodological issues*

It might be argued that the failure to find a significant anatomical overlap between CMA and CSv activations is an artefact of fMRI statistical thresholding procedures, which are sometimes overly conservative due to prioritising control of Type I error over control of Type II error. However, this is extremely unlikely to have occurred in this case due to the relatively liberal threshold employed ($Z > 1.96$).

The simple and random versions of the motor task that were contrasted with baseline to localize CMA both used auditory tones to cue participants to move. Therefore, it might be argued that the cingulate activity produced by these tasks was in whole or in part a sensory response to tones. However, this possibility can be ruled out because previous studies indicate that auditory stimulation is neither necessary nor sufficient to produce activation in the posterior cingulate. That it is not necessary is demonstrated by Amiez and Petrides (2012) who localised CMA using visual presentation of sentences to cue movement. That it is not sufficient is demonstrated by Lewis, Beauchamp, and DeYoe's (2000) report of an activation map produced by listening to auditory motion, which lacked any foci in the posterior cingulate. Furthermore, fMRI studies of tonotopic organisation in auditory cortex sometimes present whole brain analysis of the response to tones versus a resting baseline, and the results of such studies do not include cingulate activation, e.g., Wessinger, Buonocore, Kussmaul, and Mangun (1997) and Bilecen, Scheffler, Schmid, Tschopp, and Seelig (1998).

An interesting observation concerning CMA is that the three motor tasks we used, which required different types of movement, and were of differing levels of complexity all produced similar activation in CMA. This is the first study of CMA in which a high-level motor task such as the visuomotor flow-tracking used task here has been employed. The fact it produced a similar response in CMA to that produced by the simpler motor tasks suggests that CMA motor activity is low-level in nature similar to that in primary motor cortex.

4.2. *Interpretation of unanticipated findings*

One possible explanation for the finding that CSv activation failed to occur in the visuomotor condition is that participants were distracted from processing the optic flow by the joystick task, but this seems unlikely because behavioural performance in the heading tracking task was good (Fig. 5) and this could only have been achieved by using the optic flow to perform the tracking task. Therefore, our findings suggest that

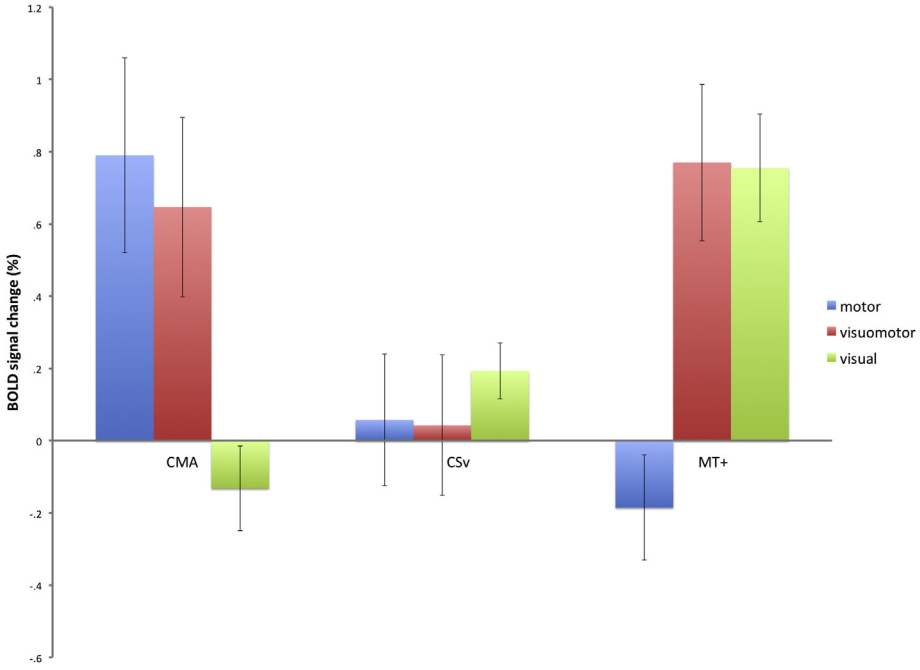

Fig. 8 – BOLD signal change broken down by experimental condition and ROI. Independent data was used for definition of ROIs and extraction of signal change. Error bars indicate 95% confidence intervals.

performing a visuomotor task related to optic flow and heading perception causes the activity in CSv to be suppressed. We offer two possible explanations for this that might be tested by future studies. One possibility is that CSv represents information from optic flow that can be used to control action by CMA and other motor areas. When this information is used, as it was in our visuomotor condition, then it is no longer relevant and the related neural activity in CSv that supports it gets suppressed. However, in the case of passive viewing, the suppression in CSV is not triggered thus resulting in more sustained neural activity that can be detected in the BOLD signal.

A second possibility is that the suppression of CSv activity in the visuomotor task might be explained by the theory that the brain creates an internal forward model of the evolving visual scene. The internal model represents the likely sensory consequences of planned actions, which are continuously compared with sensory feedback of the actual consequences of actions (e.g., Miall & Wolpert, 1996). One feature of this theory is that where sensory feedback matches the sensory consequences predicted by the forward model, the feedback 'cancels' the prediction signal, whereas when these two signals are unequal the resulting 'error signal' alerts the actor to the partial failure of their action (e.g., Blakemore, Wolpert, & Frith, 1998). In the case of the present open-loop visuomotor task the sensory feedback was not actually linked to the success or failure of action in the normal way, but could easily give the perceptual impression that the participants' joystick movements were controlling the course taken in the scene.[3] Under these unusual circumstances it is likely that the visual sensory feedback and forward model predictions were fairly similar, which according to this proposal would lead to cancellation of both signals and thus the suppression of CSv activation during visuomotor control.

To explain our results from the above theoretical standpoint, it is necessary to hypothesize that at least in the context of optic-flow and self-motion CSv is the brain region where forward model predictions and sensory feedback are integrated. Under passive viewing, because action does not occur, the forward model is not engaged leaving only the sensory optic flow signal in CSv, which is not cancelled leading to a positive BOLD response. This possibility would be consistent with the recent findings of Furlan et al. (2013) who used multivoxel pattern analysis to establish that of all the flow sensitive brain regions, CSv is the one most clearly associated with extracting a heading direction signal from optic flow. Consistent with our findings, their paradigm activated CSv using a passive viewing of optic flow task rather than a visuomotor task, and the BOLD signal in CSv was only elevated when heading direction was varying. Integrating Furlan et al.'s findings with the theoretical perspective of internal models suggests the hypothesis that CSv is the area where a forward model prediction of heading direction is integrated with sensory signals about actual heading direction.

[3] The recorded lag between joystick position and the path trajectory in the display was quite large (.75 sec, see Fig. 5), but this value is an overestimate of the real lag of hand movement to the perceived heading change for reasons given in the methods. The real lag in the current study was in the range of 220–350 ms. Previous studies have shown that participants can adapt to a 300 ms delay between joystick/hand movement and the motion of a display in the case where there is a real contingency between the two (e.g., Foulkes & Miall, 2000). Accordingly, it is natural that subjects in the current study might develop the perceptual impression of linkage between joystick movements and the tracked display.

Acknowledgements

This study was supported by a grant from the Research Grants Council of Hong Kong (<http://rcgas.hku.hk/Project/PrjDetail.aspx?prj_code=103487>HKU>748010H) to L. Li and D. T. Field. We thank two anonymous reviewers for their comments on a previous draft of the manuscript.

REFERENCES

Amiez, C., & Petrides, M. (2012). Neuroimaging evidence of the anatomo-functional organization of the human cingulate motor areas. *Cerebral Cortex, 24*(3), 563–578.

Andersson, J. L., Jenkinson, M., & Smith, S. (2007a). *Non-linear registration, aka Spatial normalisation*. FMRIB technical report TR07JA2. FMRIB Analysis Group of the University of Oxford.

Andersson, J. L., Jenkinson, M., & Smith, S. (2007b). *Non-linear optimisation*. FMRIB technical report TR07JA1. Oxford (UK): FMRIB Centre.

Antal, A., Baudewig, J., Paulus, W., & Dechent, P. (2008). The posterior cingulate cortex and planum temporale/parietal operculum are activated by coherent visual motion. *Visual Neuroscience, 25*(01), 17–26.

Behrens, T., Woolrich, M. W., & Smith, S. (2003, June). Multi-subject null hypothesis testing using a fully bayesian framework: theory. In *Annual Meeting of the Organization for Human Brain Mapping*.

Bilecen, D., Scheffler, K., Schmid, N., Tschopp, K., & Seelig, J. (1998). Tonotopic organization of the human auditory cortex as detected by BOLD-FMRI. *Hearing Research, 126*(1), 19–27.

Billington, J., Field, D. T., Wilkie, R. M., & Wann, J. P. (2010). An fMRI study of parietal cortex involvement in the visual guidance of locomotion. *Journal of Experimental Psychology: Human Perception and Performance, 36*(6), 1495.

Blakemore, S. J., Wolpert, D. M., & Frith, C. D. (1998). Central cancellation of self-produced tickle sensation. *Nature Neuroscience, 1*(7), 635–640.

Cardin, V., & Smith, A. T. (2011). Sensitivity of human visual cortical area V6 to stereoscopic depth gradients associated with self-motion. *Journal of Neurophysiology, 106*(3), 1240–1249.

Crowell, J. A., Royden, C. S., Banks, M. S., Swenson, K. H., & Sekuler, A. B. (1990). Optic flow and heading judgments [abstract]. *Investigative Ophthalmology & Visual Science, 31*(Suppl.), 522.

Deiber, M. P., Passingham, R. E., Colebatch, J. G., Friston, K. J., Nixon, P. D., & Frackowiak, R. S. J. (1991). Cortical areas and the selection of movement: a study with positron emission tomography. *Experimental Brain Research, 84*(2), 393–402.

Dumoulin, S. O., Bittar, R. G., Kabani, N. J., Baker, C. L., Le Goualher, G., Pike, G. B., et al. (2000). A new anatomical landmark for reliable identification of human area V5/MT: a quantitative analysis of sulcal patterning. *Cerebral Cortex, 10*(5), 454–463.

Field, D. T., Wilkie, R. M., & Wann, J. P. (2007). Neural systems in the visual control of steering. *The Journal of Neuroscience, 27*(30), 8002–8010.

Fischer, E., Bülthoff, H. H., Logothetis, N. K., & Bartels, A. (2012). Visual motion responses in the posterior cingulate sulcus: a comparison to V5/MT and MST. *Cerebral Cortex, 22*(4), 865–876.

Foulkes, A. J. M., & Miall, R. C. (2000). Adaptation to visual feedback delays in a human manual tracking task. *Experimental Brain Research, 131*(1), 101–110.

Furlan, M., Wann, J. P., & Smith, A. T. (2013). A representation of changing heading direction in human cortical areas pVIP and CSv. *Cerebral Cortex*. http://dx.doi.org/10.1093/cercor/bht132. bht132.

Hooge, I. T. C., Beintema, J. A., & van den Berg, A. V. (1999). Visual search of heading direction. *Experimental Brain Research, 129*(4), 615–628.

Jenkinson, M., Bannister, P., Brady, M., & Smith, S. (2002). Improved optimization for the robust and accurate linear registration and motion correction of brain images. *NeuroImage, 17*(2), 825–841.

Jenkinson, M., & Smith, S. (2001). A global optimisation method for robust affine registration of brain images. *Medical Image Analysis, 5*(2), 143–156.

Lewis, J. W., Beauchamp, M. S., & DeYoe, E. A. (2000). A comparison of visual and auditory motion processing in human cerebral cortex. *Cerebral Cortex, 10*(9), 873–888.

Li, L., & Cheng, J. C. K. (2011). Perceiving path from optic flow. *Journal of Vision, 11*(1), 1–15, 22.

Miall, R. C., & Wolpert, D. M. (1996). Forward models for physiological motor control. *Neural Networks, 9*(8), 1265–1279.

Moutsiana, C., Field, D. T., & Harris, J. P. (2011). The neural basis of centre-surround interactions in visual motion processing. *PloS One, 6*(7), e22902.

Picard, N., & Strick, P. L. (1996). Motor areas of the medial wall: a review of their location and functional activation. *Cerebral Cortex, 6*(3), 342–353.

Pitzalis, S., Sdoia, S., Bultrini, A., Committeri, G., Di Russo, F., Fattori, P., et al. (2013). Selectivity to translational egomotion in human brain motion areas. *PloS One, 8*(4), e60241.

Smith, S. M. (2002). Fast robust automated brain extraction. *Human Brain Mapping, 17*(3), 143–155.

Smith, A. T., Wall, M. B., & Thilo, K. V. (2012). Vestibular inputs to human motion-sensitive visual cortex. *Cerebral Cortex, 22*(5), 1068–1077.

Wall, M. B., & Smith, A. T. (2008). The representation of egomotion in the human brain. *Current Biology, 18*(3), 191–194.

Wessinger, C. M., Buonocore, M. H., Kussmaul, C. L., & Mangun, G. R. (1997). Tonotopy in human auditory cortex examined with functional magnetic resonance imaging. *Human Brain Mapping, 5*(1), 18–25.

Woolrich, M. W., Ripley, B. D., Brady, M., & Smith, S. M. (2001). Temporal autocorrelation in univariate linear modeling of FMRI data. *NeuroImage, 14*(6), 1370–1386.